HHS Public Access

Author manuscript

Oncogene. Author manuscript; available in PMC 2016 January 01.

Published in final edited form as:

Oncogene. 2015 July ; 34(27): 3556–3567. doi:10.1038/onc.2014.284.

The Serine Protease Inhibitor Elafin Maintains Normal Growth Control by Opposing the Mitogenic Effects of Neutrophil Elastase

Joseph A. Caruso[1,4], **Said Akli**[1], **Laura Pageon**[2], **Kelly K. Hunt**[1,3], and **Khandan Keyomarsi**[1,4]

[1]Department of Experimental Radiation Oncology, The University of Texas MD Anderson Cancer Center, Houston, Texas, USA

[2]Department of Veterinary Medicine and Surgery, The University of Texas MD Anderson Cancer Center, Houston, Texas, USA

[3]Department of Surgical Oncology, The University of Texas MD Anderson Cancer Center, Houston, Texas, USA

[4]The University of Texas Graduate School of Biomedical Sciences, Houston, Texas, USA

Abstract

The serine protease inhibitor, elafin, is a critical component of the epithelial barrier against neutrophil elastase (NE). Elafin is downregulated in the majority of breast cancer cell lines compared to normal human mammary epithelial cells (HMECs). Here, we evaluated the role of elafin and NE on proliferation and tumorigenesis. Elafin is induced in growth factor deprived HMECs as they enter a quiescent (G0) state, suggesting that elafin is a counterbalance against the mitogenic effects of NE in G0 HMECs. Stable knockdown of elafin compromises the ability of HMECs to maintain G0-arrest during long-term growth factor deprivation; this effect can be reversed by re-expression of wild-type elafin, but not elafin-M25G lacking protease inhibitory function. These results suggest that NE, which is largely contributed by activated neutrophils in the tumor microenvironment, may be negatively regulating the ability of elafin to arrest cells in G0. In fact when purified NE was added to elafin knockdown HMECs, these cells demonstrated greater sensitivity to the growth promoting effects of purified NE. Activation of ERK signaling, downstream of toll-like receptor 4, was essential to the mitogenic effect of NE on HMECs. These findings were next translated to patient samples, and immunohistochemical analysis of normal breast tissue revealed robust elafin expression in the mammary epithelium; however, elafin expression was dramatically downregulated in a significant proportion of human breast tumor specimens. The loss of elafin expression during breast cancer progression may promote tumor growth as a consequence of increased NE-activity. To address the role of NE in mammary

To whom correspondence should be addressed: Khandan Keyomarsi, Ph.D., Experimental Radiation Oncology, The University of Texas MD Anderson Cancer Center, 1515 Holcombe Blvd., Box 66, Houston, TX 77030-4095. Tel.: 713-792-4845; Fax: 713-794-5369; kkeyomar@mdanderson.org.

Conflict of Interest: The authors of this manuscript declare no conflicts of interest.

tumorigenesis, we next examined if deregulated NE-activity enhances mammary tumor growth. NE knockout in the C3(1)TAg mouse model of mammary tumorigenesis suppressed proliferation and reduced the kinetics of tumor growth. Overall, the imbalance between NE and its inhibitors, such as elafin, presents an important therapeutic target in breast cancer.

Keywords

Elafin; Neutrophil Elastase; Human Mammary Epithelial Cells; Quiescence; Proliferation

Introduction

Elafin, an endogenous serine protease inhibitor, is an important component of the epithelial shield against excessive neutrophil elastase (NE) activity (1). NE, a potent serine protease, is normally synthesized in the bone marrow and sequestered within the azurophilic granules of neutrophils. The major physiological function of NE is the intracellular destruction of pathogens following phagocytosis at sites of infection (2). Activated neutrophils also secrete NE into the extracellular environment. In this context, NE has important roles in the antimicrobial, inflammatory, and wound healing responses. Under normal physiological conditions, serine protease inhibitors, including elafin, rapidly quench NE activity, contributing to the resolution of inflammation and preserving tissue integrity (3). Imbalance between NE and its inhibitors is implicated in the pathogenesis of a wide range of diseases characterized by excessive or chronic inflammation (4).

Elafin downregulation was observed in several inflammatory diseases, including acute respiratory distress syndrome (5), inflammatory bowel disease (6), and acute lung injury (7). In these studies, elafin downregulation correlates with increased NE activity and disease progression. In mouse models, constitutive elafin overexpression protected against acute lung injury (8), reduced pulmonary hypertension following chronic hypoxia (9), diminished tissue destruction associated with experimental colitis (6), and improved heart function after viral myocarditis (10) or myocardial infarction (11). The available evidence supports an important role for elafin in suppressing NE-activity and mitigating the pathogenesis of inflammatory disease.

Several studies suggest that loss of elafin-mediated control of NE activity is a feature of malignant growth. Elafin downregulation was observed in poorly-differentiated compared to well-differentiated squamous cell carcinomas (12, 13). Elafin expression is lost in melanoma and breast cancer cell lines compared to normal melanocytes and human mammary epithelial cells (HMECs) (14, 15). The transcription factor C/EBPβ is required for elafin expression in HMECs. Accumulation of a truncated, dominant-negative isoform of C/EBPβ accounts for elafin downregulation in breast cancer cell lines (16). We previously reported that ectopic expression of elafin induced apoptosis in Rb negative and growth arrest in Rb-positive breast cancer cell lines (17), suggesting that elafin has tumor suppressive properties in the context of breast cancer.

In the present study, we initially sought to understand the normal regulation and role of endogenously expressed elafin in HMECs, as well as the consequence of elafin

downregulation on critical aspects of tumorigenesis. We observed dramatic upregulation of elafin in quiescence (G0) HMECs, leading us to hypothesize that elafin is a critical counterbalance against the mitogenic effects of NE. Using HMECs as a model system, the results support a role for elafin in opposing the NE-induced proliferation. We observed dramatic downregulation of elafin expression in patient-derived breast tumor specimens compared to elafin expression in the normal mammary epithelium, suggesting compromised control of NE-activity is indeed a feature of breast tumorigenesis. Finally, we investigated the implications of deregulated NE-activity on tumor growth in the C3(1)TAg mouse model of mammary tumorigenesis. In this model, NE knockout significantly reduced tumor growth and proliferation. A therapeutic approach designed to restore appropriate control of NE-activity may lead to the inhibition of tumor growth in breast cancer patients.

Results

Elafin is Highly Expressed in Quiescent HMECs

Primary (i.e mortal) 81N, 70N, and 76N HMECs were cultured under growth factor-deficient conditions and harvested at 6-hour intervals for 48 hours to examine the expression of endogenous elafin during growth arrest. DNA content analysis revealed that HMECs were progressively arrested in G0/G1 phase. Complete arrest was observed between 24 and 36 hours of continuous culture (Figure 1A). Western blot analysis showed dramatic upregulation of elafin over the growth factor deprivation time course (Figure 1B), corresponding to the accumulation of HMECs in G0/G1 phase. Immunofluorescence analysis of Ki67, which is specifically downregulated in quiescent (G0) cells (18), confirms that growth factor deprivation induces G0 (and not G1) arrest in HMECs (Figure 1C). Elafin immunofluorescence demonstrates increased cytoplasmic staining intensity following growth factor deprivation (Figure 1D).

Elafin has primarily been characterized as a secreted protein; therefore we next examined elafin levels in conditioned media by ELISA. The concentration of elafin in the conditioned media of 81N, 70N, and 76N HMECs cultured in the presence of growth factors for 24 hours was 2.6–2.9 ng/mL. Significantly higher concentrations of elafin were observed in HMECs cultured in growth factor-deprived medium: 4.0–6.3 ng/mL at 24 hours and 7.1–11.5 ng/mL at 48 hours (Figure 1E).

Quantitative RT-PCR (qPCR) analysis revealed that elafin is highly induced at the mRNA level under growth factor deprivation conditions, increasing 12- to 178-fold at 24 hours and 165- to 240-fold at 48 hours compared to the level of elafin mRNA in HMECs cultured in growth factor-containing medium (Figure 1F).

Previously, we reported that accumulation of a truncated, dominant negative isoform of C/EBPβ represses elafin expression in breast cancer cell lines (16). We next interrogated if C/EBPβ elements in the elafin promoter are necessary for elafin upregulation in G0 HMECs by luciferase reporter analysis of the elafin promoter. The results revealed that elafin upregulation in HMECs was dependent on C/EBPβ sites 4 and 5, which we previously identified (16) (Figure S1A). Lastly, in the immortalized HMECs 76NF2V, knockdown of

C/EBPβ (Figure S1B) prevented elafin upregulation following growth factor deprivation (Figure S1C).

Rb-Deficient HMECs are Incapable of G0 Arrest and Fail to Upregulate Elafin

To determine if Rb-dependent G0-arrest is required for elafin expression, we examined a panel of immortalized HMECs (19) that express both p53 and Rb (76NF2V), lack p53 (76NE6), or lack Rb and related pocket proteins (76NE7). Growth factor deprivation (GFD) for 48 hours resulted in the downregulation of Ki67 in 76NE6 and 76NF2V cells but not 76NE7 cells (Figure 2A). Maintenance of Ki67 expression in growth factor-deprived 76NE7 cells confirmed that loss of the Rb checkpoint eliminates the ability of HMECs to arrest in G0. 76NE6 and 76NF2V progressively arrested in G0/G1 over the 48-hour GFD time course and upregulated elafin (Figure S2, A and B), similar to primary HMECs (Figure 1, A and B). 76NE7 cells were incapable of elafin upregulation compared to 76NE6 and 76NF2V cells (Figure 2B) and they arrested in the G2-phase (not G1 phase) of the cell cycle over the 48-hour GFD time-course (Figure S2A). Furthermore, immortalized HMECs asynchronously proliferating or arrested in the G1-phase following treatment with lovastatin, S-phase following treatment with aphidicolin, or G2/M phase following treatment with nocodazole were unable to upregulate elafin compared to growth factor deprived, G0-arrested 76NE6 and 76NF2V; Rb-deficient 76NE7 cells were unable to upregulate elafin in response to any of the conditions examined (Figure 2C).

Similar results were obtained using the immortalized 81N HMEC system; Rb-deficient 81NE7 HMECs accumulated in the G2 phase of the cell cycle (Figure S2C) and cannot upregulate elafin (Figure S2D) following GFD, compared to Rb-expressing 81NE6 and parental 81N HMECs. Furthermore, Rb knockdown renders 76NF2V and 76NE6 incapable of arrest in G0/G1 phase (Figure 2D) and elafin upregulation (Figure 2E) following GFD.

Taken together, these results demonstrated that Rb-dependent G0 arrest is required for elafin upregulation in growth factor deprived HMECs, suggesting a role for elafin in growth control.

Elafin Knockdown HMECs Circumvent G0 Arrest and Proliferate in the Absence of Growth Factors

To examine the role of elafin in maintenance of G0 arrest, elafin was knocked-down in 76NE6 (Figure 3A) and 81NE6 (Figure S3A) HMECs and the kinetics of cell proliferation were assessed under growth factor-deficient conditions (Figure 3B). Since FBS contains an abundance of serine protease inhibitors, cells were cultured in media lacking supplemental FBS. Both 76NE6 and 81NE6 elafin-knockdown cell lines exhibited modest but significant growth factor-independent proliferation with doubling times between 66 and 81 hours, while control cells exhibited complete growth cessation after only 24 hours in growth factor-depleted medium (Figure 3C).

To verify the specificity of elafin knockdown and examine the importance of elafin-mediated protease inhibition in this system, we complemented 76NE6 elafin-knockdown cells with wild-type elafin (sensitive to shRNA downregulation), shRNA-resistant-elafin, and shRNA-resistant-M25G-elafin (the M25G mutation inactivates the protease inhibitor

domain) (20) (Figures 3D and S3B). Elafin-knockdown 76NE6 cells demonstrated an approximate doubling in cell number compared to controls following 144 hours of growth factor deprivation (Figure 3E). Complementation of elafin-knockdown 76NE6 cells with wild-type elafin, but not M25G-elafin, reduced cell number to the level of controls (Figure 3E). These experiments revealed a critical role of elafin-mediated protease inhibition in the maintenance of G0 arrest.

Elafin Knockdown HMECs Demonstrate Enhanced Sensitivity to the Growth-Promoting Effect of Exogenous NE

The inability of elafin-M25G to inhibit the growth factor independent proliferation of elafin knockdown HMECs (Figure 3E) suggests a critical role for its deregulated protease activity. Notably, the level of growth factor independent proliferation observed in elafin knockdown HMECs was modest (Figure 3C) consistent with the relatively low levels of NE activity in these cells (21). Since in the tumor microenvironment the majority of NE is contributed by activated neutrophils (22, 23), we next interrogated the ability of exogenous NE to induce the proliferation of elafin knockdown HMECs (Figure 4). In this experiment, elafin-knockdown and control 76NE6 cells were growth factor deprived for 24 hours, and purified NE was added directly to the media as described (24). Cell density was measured using the MTT assay 48 hours after addition of NE (Figure 4A). Compared to controls, the elafin-knockdown 76NE6 cells stimulated with NE at concentrations of 1–8 nM demonstrated significantly greater sensitivity to the growth promoting effect of exogenous NE (Figure 4B).

The ability of NE to induce proliferation was dose-dependent. Elafin-knockdown 76NE6 cells were sensitive to the growth-promoting effect of 2 nM NE, whereas elafin-expressing controls were not (Figure 4C). Complementation of elafin-knockdown 76NE6 cells with shRNA-resistant-elafin, but not shRNA-resistant-M25G-elafin, attenuated proliferation induced by 2 nM NE (Figure 4C). No differences were observed in this experiment between groups not treated with NE because cell number was assessed following only 72 hours of growth factor deprivation. [Significant differences in cell number were not seen in elafin-knockdown HMECs until 120 hours of growth factor deprivation (Figure 3C).] Pharmacological inhibitors of NE activity sivelestat and GW311616 inhibited NE-induced proliferation in 76NE6 cells (Figure S4, A and B); further evidencing that the mitogenic-effect of NE is dependent on NE-activity and not contaminants in the NE preparation.

These findings provided evidence that elafin is an important component of the epithelial shield against deregulated NE activity.

NE Induces Proliferation through TLR4-Dependent Activation of ERK Signaling

Microarray analysis identified differentially expressed genes between elafin-knockdown and control 76NE6 cells following 0, 48, and 168 hours of growth factor deprivation (Figure S5A). Upregulation of the immediate early response gene, EGR1, at the 48-hour time point was of particular interest given the previously identified role of EGR1 in cell cycle re-entry of G0-arrested HMECs (25, 26). We validated the upregulation of EGR1 in 76NE6 elafin-knockdown cells by qPCR (Figure S5B).

The ERK signaling pathway is known to control EGR1 transcription (26). Addition of NE (10nM) to growth factor deprived 76NE6 cells resulted in activation of ERK phosphorylation that peaked within 15 to 30 minutes (Figure S6A). Upregulation of ERK target genes EGR1 and FOS were observed 3 hours after the addition of NE to growth-arrested 76NE6 cells (Figure S6B). Addition of the MEK1/2 selective inhibitor U0126 and MEK1 siRNA effectively inhibited ERK phosphorylation following the addition of NE to growth-arrested 76NE6 cells (Figure S6C) and consistently attenuated NE-induced proliferation (Figure S6, D and E).

Given the rapidity of ERK activation following the addition of NE, we hypothesized that an extracellular receptor mediates the mitogenic effect of NE on HMECs. TLR4 (27), PAR2 (28), and EGFR (29) have all been implicated in NE-induced ERK activation. We observed that knockdown of TLR4 reproducibly abrogated ERK activation in growth factor-deprived 76NE6 and 81NE6 cells (Figure 4D) following the addition of 10 nM NE (sufficient to overwhelm endogenous elafin and induce maximal proliferation in both 76NE6 and 81NE6 cells) and attenuated NE-induced proliferation (Figure 6E).

These findings suggested that the mitogenic activity of NE in quiescent HMECs is dependent on TLR4-induced ERK activation.

Elafin is Downregulated in Breast Tumor Specimens Compared to the Normal Mammary Epithelium

To examine the physiological relevance of elafin expression in human breast cancer, we initially measured elafin protein levels in 36 breast cancer cell lines and found that elafin expression was absent from all breast tumor cell lines examined as compared to 76NE6 cells (Figure 5A).

Next, we translated these *in vitro* findings to patient-derived tissue specimens, where we examined elafin expression by IHC in normal breast tissue from reduction mammoplasty (n=15) and invasive breast carcinoma (n=202) using a highly specific monoclonal antibody against elafin (Hycult, clone: TRAB/2F) (30). Based on the absence of elafin in breast cancer cell lines, we hypothesized that elafin expression is downregulated in human breast cancer specimens compared to the normal mammary epithelium. Supporting our hypothesis, elafin was expressed within the epithelial compartment of the normal mammary gland (Figure 5B), but was absent from the epithelial component of human breast tumors (Figure 5C). In some cases, infiltrating leukocytes in the tumor microenvironment expressed high levels of elafin contrasting with the absence of elafin within the tumor epithelium (Figure 5C). Quantification revealed a significantly lower frequency of elafin positive cells in breast tumors specimens compared the normal mammary epithelium (Figure 5D).

Our IHC analysis revealed that elafin was significantly downregulated in human breast tumors, suggesting that the epithelial shield against NE-activity is compromised during breast tumorigenesis.

NE Knockout Reduces Tumor Growth and Proliferation in the C3(1)TAg Model of TNBC

Next, we set out to understand the significance of deregulated NE-activity in a mouse model of breast tumorigenesis. We hypothesized that deregulated NE is capable of promoting breast tumor growth. Given the correlation between high levels of NE and ER/PR-negative status (31), we chose to test this hypothesis in a mouse model of triple-receptor negative breast cancer (TNBC). The C3(1)TAg mouse model has been shown to give rise to TNBC and is molecularly similar to basal-like breast cancer in humans (32–35). C3(1)TAg mice were crossed with the previously established NE knockout mice (2), both were maintained in the FVB/N background (Figure S7).

C3(1)TAg x NE+/+ and C3(1)TAg x NE−/− cohorts were followed for tumor initiation and growth was followed until the tumor exceeded the maximal allowable size based on the requirements of the institutional review board. The doubling time of each tumor was calculated by application of the exponential growth model. Tumors in NE−/− mice demonstrated a significantly slower growth rate compared to tumors in NE+/+ mice (Figure 6A). To determine if the difference in the tumor growth rate was due to altered proliferation, tumors were subjected to qPCR analysis of the proliferation markers Mki67 and Melk (Figure 6B) and IHC analysis of BrdU incorporation (Figure 6C). The mRNA levels of both Mki67 and Melk were significantly suppressed in C3(1)TAg x NE−/− genotype tumors compared to C3(1)TAg x NE+/+ genotype tumors (Figure 6B). Significantly less BrdU incorporation was observed in tumors arising in NE−/− genotype mice compared to tumors arising in NE+/+ genotype mice (Figure 6D). IHC analysis of BrdU incorporation was also performed on the contralateral mammary gland of tumor bearing mice (Figure 6E). Quantification revealed significantly lower levels of proliferation in the mammary glands of C3(1)TAg x NE−/− genotype mice compared to C3(1)TAg x NE+/+ genotype mice (Figure 6F). The results presented here are consistent with decreased proliferation in C3(1)TAg x NE−/− genotype tumors compared to C3(1)TAg x NE+/+ genotype tumors. Overall, the data presented here provides direct *in vivo* evidence that NE enhances tumor growth in a mouse model of TNBC.

Discussion

In this study, we examined the regulation/role of endogenously expressed elafin and the consequence of deregulated NE-activity on proliferation and tumor growth. Initially, we observed that elafin is upregulated at the transcription level in G0 HMECs (Figure 1F), which resulted in its intracellular accumulation (Figure 1B) and increased secretion into conditioned media (Figure 1E). Elafin transactivation required the transcription factor C/EBPβ (Figure S1) and Rb-dependent cell cycle checkpoint control (Figure 2). Rb and C/EBPβ are essential to the control of proliferation and differentiation within the mammary gland (36, 37). Physical interaction with Rb was previously shown to be critical for C/EBPβ DNA binding (38) and may play a role in the regulation of elafin expression in HMECs. The Rb and C/EBPβ pathways are commonly deregulated in human cancers, likely accounting for elafin downregulation during breast tumorigenesis (16, 39)

The upregulation of elafin in G0 HMECs (Figure 1) suggested a role for elafin in normal growth control. Elafin is an important component of the epithelial shield against excessive

NE activity (1). The conventionally understood role of deregulated NE activity in tumor progression is promotion of cell invasion and metastasis through extracellular matrix degradation and the cleavage of adhesion molecules (40). However, several NE-specific substrates have recently been identified with important roles in cell proliferation. For example, NE-mediated degradation of insulin receptor substrate-1 (IRS-1) increased phosphoinositide 3-kinase (PI3K) activity such that NE knockout reduced downstream Akt activation and tumor cell proliferation in the *loxP*-Stop-*loxP* K-ras^{G12D} mouse model of lung cancer, (22). NE was also been implicated in cleavage of cyclin E into low-molecular weight isoforms capable of hyperactivating cyclin-dependent kinase 2, enhancing cell proliferation and inducing tumor formation in mouse models (41, 42).

We hypothesized that elafin is an important counterbalance against the mitogenic effects of NE-activity. Elafin knockdown HMECs proliferated in the absence of growth factors (Figure 3C). This effect could be ameliorated by reconstitution of wild type but not protease inhibitor domain mutant elafin, suggesting that deregulated serine protease activity underlies growth factor independent proliferation in elafin knockdown HMECs (Figure 3E). The level of proliferation observed in elafin knockdown HMECs was relatively modest and only evident following prolonged growth factor deprivation, consistent with the relatively low levels of NE activity in this HMEC system (21). In the tumor microenvironment, the majority of NE is contributed by activated neutrophils (23). To model this, we added purified NE to the growth factor deficient culture medium of HMECs, resulting in a robust, dose-dependent increase in cell proliferation. In this system, elafin knockdown HMECs demonstrated increased sensitivity to the mitogenic effect of NE compared to elafin expressing controls (Figures 4B).

In models of inflammatory disease, the addition of exogenous NE enhanced cell proliferation both *in vitro* and *in vivo* (24, 43, 44). The concentrations of NE resulting in a physiological response *in vitro* varies between studies; proliferation was induced in airway smooth muscle cell by addition of 0.35–1.7 nM NE (44), in keratinocytes by addition of 0.1–33 nM NE (24), and in lung fibroblasts by addition of 3.5–862 nM NE (29). In the present study, the concentrations of NE utilized to induce proliferation in HMECs ranged from 1–10 nM, which is comparable to previously published studies. Possible explanations for the variability in NE-concentration required to induce cell proliferation *in vitro* include: differences in the source/activity of the NE, the sensitivity of the cell lines, and the concentration of exogenous serine protease inhibitors in the culture medium.

In our HMEC system, we found that activation of the ERK signaling pathway (Figure S6A) was required for the mitogenic effect of NE on HMECs (Figure S6D). This observation was consistent with previous reports demonstrating the activation of ERK signaling following addition of exogenous NE (29). NE-induced activation of TLR4 was previously reported (27). In our HMEC model system, knockdown of TLR4 completely inhibited NE-induced ERK activation (Figure 4D) and proliferation (Figure 4E). Breast tumor cell lines are known to express TLR4 (45), suggesting that deregulated NE activity may be an important endogenous activator of TLR4, downstream ERK signaling, and proliferation throughout breast tumorigenesis. We have also examined the ERK signaling pathway is breast cancer patients and find that NE positive tumor associated neutrophils correlate with the

phosphorylation of ERK effector p90RSK and Rb (not shown), recapitulating our cell line data presented here.

In this study, we demonstrate for the first time that elafin is indeed downregulated during breast tumorigenesis through IHC-analysis of patient-derived normal and malignant breast tissue (Figure 5D). Our *in vitro* results suggest that loss of elafin eliminates a critical counterbalance against the mitogenic effect of deregulated NE-activity. However, *in vitro* studies fail to completely recapitulate the complex interactions between the tumor epithelial and stromal compartments. We used the C3 (1) TAG mouse model to directly investigate the role of NE in proliferation and found that, NE knockout in the C3(1)TAg mouse model of mammary tumorigenesis suppressed proliferation (Figure 6D) and reduced the kinetics of tumor growth (Figure 6A) compared to NE expressing controls.

Extensive experimental evidence has demonstrated that the ability of tumor cells to recruit and manipulate non-malignant cell types, including leukocytes, governs their malignant growth potential. The cellular constituents of the tumor stroma are not susceptible to many of the selective pressures driving therapeutic resistance in tumor cells. Therefore therapeutic modalities targeting critical microenvironmental mediators of tumor progression may yield durable anti-tumor responses alone or in combination with existing therapies. Pharmacological inhibitors of NE have been developed for the treatment of inflammatory lung disease (46) and could be evaluated as a therapeutic approach to reduce breast tumor growth.

Materials and Methods

Cell Lines and Culture Conditions

Primary HMECs 70N, 76N, and 81N isolated from reduction mammoplasty samples and immortalized derivatives were obtained from Dr. V. Band and culture conditions are as described. (19).

Lentiviral shRNA

Target-specific shRNA was obtained in the pGIPZ lentiviral vector system (OpenBiosystems) from the MD Anderson shRNA and ORFeome Core Facility. Lentiviral packaging was performed in HEK-293T cells using the pCMV deltaR8.2 and pMD2.G vectors produced by the Didier Trono laboratory and made available through the Addgene repository. Target cells were infected with the virus-containing medium in the presence of 8 μg/mL polybrene.

Complementation of Elafin-Knockdown Cells

Elafin cDNA was cloned into the pDONR201 vector via the gateway BP clonase (Invitrogen). To create shRNA-resistant elafin, three consecutive codons along the shRNA targeting region were mutated at the wobble position using the Quikchange Lightning site-directed mutagenesis kit (Stratagene). The M25G mutation to the protease inhibitor domain (20) was created via the same method. All primer sequences are available in supplemental information. Following sequence validation, elafin pENTR vectors were cloned into the

plenti CMV Blast DEST vector (Eric Campeau lab, obtained from the Addgene repository) using LR clonase (Invitrogen). Viral packaging was performed as described for lentiviral shRNA vectors. Elafin shRNA cells were infected with elafin containing plenti CMV vectors and selected in 20 μg/ml blasticidin and 1 μg/ml puromycin.

Antibodies for Western Blot Analysis

Mouse monoclonal antibodies to elafin (clone: TRAB/2F, HyCult), total Rb (BD Biosciences), p53 (Calbiochem), ERK (clone: L34F12; Cell Signaling Technology), and actin (Chemicon); rabbit polyclonal antibody to phospho-Rb site Ser780 (Cell Signaling Technology) and TLR4 (H-80; Santa Cruz Biotechnology); and the rabbit monoclonal antibody to phospho-ERK (clone: D13.14.4E; Cell Signaling Technology).

ELISA

Immuno MaxiSorp U96 plates (Nunc) were coated with elafin polyclonal antibody (Hycult) at a concentration of 10 μg/mL diluted in 0.1 M sodium bicarbonate overnight at 4°C. The plate was blocked in 1 μg/mL BSA (Sigma) in PBS (4 hours) prior to incubation with 200 μL of conditioned medium or serially diluted recombinant elafin (Calbiochem) as a control. The antibody used to detect elafin was clone TRAF/2O (Hycult) diluted to a concentration of 50 ng/mL. The secondary antibody used was 50 ng/mL goat anti–mouse IgG HRP conjugated (Thermo). The ELISA was developed using 1-Step Ultra TMB (Thermo), the reaction was quenched with 2 M phosphoric acid, and absorbance was measured at 450 nM.

Patient Samples

IHC examination of NE was performed on specimens from 220 breast cancer patients with stage I–III disease. These patients were enrolled in a prospective study between January 2000 and June 2010 (MD Anderson lab protocol 00222). The MD Anderson Institutional Review Board approved the use of all patient derived tissues and data.

Immunohistochemistry

Deparaffinized slides were subjected to heat-induced antigen retrieval using citrate buffer (Vector). Endogenous peroxidases were quenched in 3% H_2O_2, and the sections were blocked with 1.5% normal goat serum and incubated overnight at 4°C with primary antibody: mouse monoclonal antibody to elafin (clone TRAB/2F; Hycult) diluted 1:200, rat monoclonal antibody to BrdU (clone BU1/75 [ICR1]; AbD Serotec) diluted 1:1000, and rat monoclonal antibody to Ly6G ([Gr-1] clone 1A8; BD Biosciences) diluted 1:1000. Slides were developed using the VECTASTAIN Elite ABC Kit (mouse or rabbit IgG) followed by DAB substrate (Vector) and counterstained with hematoxylin (DAKO). For BrdU and Ly6G primary antibodies, biotin-conjugated rabbit-anti-rat secondary antibody (Abcam) was substituted for the secondary goat anti-mouse antibody included in the VECTASTAIN kit at a concentration of 1:2000. Evaluation was performed with a Leica DM light microscope using the 40x optical lens. Image acquisition was performed using a SPOT Imaging Solutions camera and SPOT Advanced software.

Mice

The generation of C3(1)TAg (32) and NE knockout (2) mice were previously described. The NE knockout mice, originally in C57BL/6 were backcrossed to FVB/N strain of mice (same as the C3(1)Tag) for 12 generations. Tumors arising in the C3(1)TAg x NE−/− and C3(1)TAg x NE+/+ virgin female mice were measured bi-weekly using Vernier caliper. Mice were sacrificed, according to institutional guidelines, when tumor reached the maximum allowable size. Two hours prior to sacrifice the mice were injected intraperitoneally with 100 mg BrdU/kg body weight. The tumor was excised, half was fixed in formalin and paraffin embedding for IHC analysis and the other half was snap frozen in liquid nitrogen for mRNA extraction. The contralateral mammary gland was fixed in formalin and paraffin embedding for IHC analysis.

Statistical Considerations

All experiments were performed at least in triplicate. The results of each experiment are reported as the mean of experimental replicates. Error bars represent the standard deviation from the mean. If not otherwise indicated, pairwise comparisons were analyzed using the unpaired 2-sided *t*-test (GraphPad Prism). For all tests, $p<0.05$ was considered significant.

Supplementary Material

Refer to Web version on PubMed Central for supplementary material.

Acknowledgments

We thank Dr. Elizabeth Mittendorf discussions during the course of this study; Dr. Vimla Band for HMECs; Dr. Eric Campeau and Dr. Didier Trono for making plasmids available through the Addgene repository; Wendy Schober and Dr. Jared Burks for assistance with flow cytometry and cellular imaging; and Stephanie Deming for editorial assistance with the manuscript. This work was supported by the National Institutes of Health through MD Anderson's Cancer Center Support Grant, CA016672 and grant 5R01CA087548-10 (to KK).

References

1. Wiedow O, Schroder JM, Gregory H, Young JA, Christophers E. Elafin: an elastase-specific inhibitor of human skin. Purification, characterization, and complete amino acid sequence. J Biol Chem. 1990 Sep 5; 265(25):14791–5. [PubMed: 2394696]
2. Belaaouaj A, McCarthy R, Baumann M, Gao Z, Ley TJ, Abraham SN, et al. Mice lacking neutrophil elastase reveal impaired host defense against gram negative bacterial sepsis. Nat Med. 1998 May; 4(5):615–8. [PubMed: 9585238]
3. Korkmaz B, Moreau T, Gauthier F. Neutrophil elastase, proteinase 3 and cathepsin G: physicochemical properties, activity and physiopathological functions. Biochimie. 2008 Feb; 90(2): 227–42. [PubMed: 18021746]
4. Korkmaz B, Horwitz MS, Jenne DE, Gauthier F. Neutrophil elastase, proteinase 3, and cathepsin G as therapeutic targets in human diseases. Pharmacol Rev. 2010 Dec; 62(4):726–59. Epub 2010/11/17. eng. [PubMed: 21079042]
5. Wang Z, Chen F, Zhai R, Zhang L, Su L, Lin X, et al. Plasma neutrophil elastase and elafin imbalance is associated with acute respiratory distress syndrome (ARDS) development. PLoS One. 2009; 4(2):e4380. Epub 2009/02/07. eng. [PubMed: 19197381]
6. Motta JP, Bermudez-Humaran LG, Deraison C, Martin L, Rolland C, Rousset P, et al. Food-grade bacteria expressing elafin protect against inflammation and restore colon homeostasis. Sci Transl Med. 2012 Oct 31.4(158):158ra44. Epub 2012/11/02. eng.

7. Kerrin A, Weldon S, Chung AH, Craig T, Simpson AJ, O'Kane CM, et al. Proteolytic cleavage of elafin by 20S proteasome may contribute to inflammation in acute lung injury. Thorax. 2013 Apr; 68(4):315–21. Epub 2012/12/18. eng. [PubMed: 23242946]

8. Simpson AJ, Wallace WA, Marsden ME, Govan JR, Porteous DJ, Haslett C, et al. Adenoviral augmentation of elafin protects the lung against acute injury mediated by activated neutrophils and bacterial infection. J Immunol. 2001 Aug 1; 167(3):1778–86. Epub 2001/07/24. eng. [PubMed: 11466403]

9. Zaidi SH, You XM, Ciura S, Husain M, Rabinovitch M. Overexpression of the serine elastase inhibitor elafin protects transgenic mice from hypoxic pulmonary hypertension. Circulation. 2002 Jan 29; 105(4):516–21. Epub 2002/01/30. eng. [PubMed: 11815437]

10. Zaidi SH, Hui CC, Cheah AY, You XM, Husain M, Rabinovitch M. Targeted overexpression of elafin protects mice against cardiac dysfunction and mortality following viral myocarditis. J Clin Invest. 1999 Apr; 103(8):1211–9. Epub 1999/04/20. eng. [PubMed: 10207173]

11. Ohta K, Nakajima T, Cheah AY, Zaidi SH, Kaviani N, Dawood F, et al. Elafin-overexpressing mice have improved cardiac function after myocardial infarction. Am J Physiol Heart Circ Physiol. 2004 Jul; 287(1):H286–92. Epub 2003/12/25. eng. [PubMed: 14693682]

12. Yamamoto S, Egami H, Kurizaki T, Ohmachi H, Hayashi N, Okino T, et al. Immunohistochemical expression of SKALP/elafin in squamous cell carcinoma of the oesophagus. Br J Cancer. 1997; 76(8):1081–6. Epub 1997/01/01. [PubMed: 9376270]

13. Westin U, Nystrom M, Ljungcrantz I, Eriksson B, Ohlsson K. The presence of elafin, SLPI, IL1-RA and STNFalpha RI in head and neck squamous cell carcinomas and their relation to the degree of tumour differentiation. Mediators Inflamm. 2002 Feb; 11(1):7–12. [PubMed: 11926597]

14. Zhang M, Zou Z, Maass N, Sager R. Differential expression of elafin in human normal mammary epithelial cells and carcinomas is regulated at the transcriptional level. Cancer Res. 1995 Jun 15; 55(12):2537–41. [PubMed: 7780965]

15. Yu KS, Jo JY, Kim SJ, Lee Y, Bae JH, Chung YH, et al. Epigenetic regulation of the transcription factor Foxa2 directs differential elafin expression in melanocytes and melanoma cells. Biochem Biophys Res Commun. 2011 Apr 29; 408(1):160–6. Epub 2011/04/07. eng. [PubMed: 21466784]

16. Yokota T, Bui T, Liu Y, Yi M, Hunt KK, Keyomarsi K. Differential regulation of elafin in normal and tumor-derived mammary epithelial cells is mediated by CCAAT/enhancer binding protein beta. Cancer Res. 2007 Dec 1; 67(23):11272–83. [PubMed: 18056453]

17. Caruso JA, Hunt KK, Keyomarsi K. The neutrophil elastase inhibitor elafin triggers rb-mediated growth arrest and caspase-dependent apoptosis in breast cancer. Cancer Res. 2010 Sep 15; 70(18): 7125–36. Epub 2010/09/09. [PubMed: 20823156]

18. Keyomarsi K, Sandoval L, Band V, Pardee AB. Synchronization of tumor and normal cells from G1 to multiple cell cycles by lovastatin. Cancer Res. 1991 Jul 1; 51(13):3602–9. [PubMed: 1711413]

19. Band V, Zajchowski D, Kulesa V, Sager R. Human papilloma virus DNAs immortalize normal human mammary epithelial cells and reduce their growth factor requirements. Proc Natl Acad Sci U S A. 1990 Jan; 87(1):463–7. [PubMed: 2153303]

20. Doucet A, Bouchard D, Janelle MF, Bellemare A, Gagne S, Tremblay GM, et al. Characterization of human pre-elafin mutants: full antipeptidase activity is essential to preserve lung tissue integrity in experimental emphysema. Biochem J. 2007 Aug 1; 405(3):455–63. Epub 2007/05/11. eng. [PubMed: 17489739]

21. Hunt KK, Wingate H, Yokota T, Liu Y, Mills GB, Zhang F, et al. Elafin, an inhibitor of elastase, is a prognostic indicator in breast cancer. Breast Cancer Res. 2013 Jan 15.15(1):R3. Epub 2013/01/17. Eng. [PubMed: 23320734]

22. Houghton AM, Rzymkiewicz DM, Ji H, Gregory AD, Egea EE, Metz HE, et al. Neutrophil elastase-mediated degradation of IRS-1 accelerates lung tumor growth. Nat Med. 2010 Jan 17. Epub 2010/01/19.

23. Mittendorf EA, Alatrash G, Qiao N, Wu Y, Sukhumalchandra P, St John LS, et al. Breast cancer cell uptake of the inflammatory mediator neutrophil elastase triggers an anticancer adaptive immune response. Cancer Res. 2012 Jul 1; 72(13):3153–62. Epub 2012/05/09. eng. [PubMed: 22564522]

24. Rogalski C, Meyer-Hoffert U, Proksch E, Wiedow O. Human leukocyte elastase induces keratinocyte proliferation in vitro and in vivo. J Invest Dermatol. 2002 Jan; 118(1):49–54. Epub 2002/02/20. eng. [PubMed: 11851875]
25. Molnar G, Crozat A, Pardee AB. The immediate-early gene Egr-1 regulates the activity of the thymidine kinase promoter at the G0-to-G1 transition of the cell cycle. Mol Cell Biol. 1994 Aug; 14(8):5242–8. Epub 1994/08/01. eng. [PubMed: 8035803]
26. Zwang Y, Sas-Chen A, Drier Y, Shay T, Avraham R, Lauriola M, et al. Two phases of mitogenic signaling unveil roles for p53 and EGR1 in elimination of inconsistent growth signals. Mol Cell. May 20; 42(4):524–35. Epub 2011/05/21. eng. [PubMed: 21596316]
27. Devaney JM, Greene CM, Taggart CC, Carroll TP, O'Neill SJ, McElvaney NG. Neutrophil elastase up-regulates interleukin-8 via toll-like receptor 4. FEBS Lett. 2003 Jun 5; 544(1–3):129–32. Epub 2003/06/05. eng. [PubMed: 12782302]
28. Ramachandran R, Mihara K, Chung H, Renaux B, Lau CS, Muruve DA, et al. Neutrophil elastase acts as a biased agonist for proteinase-activated receptor-2 (PAR2). J Biol Chem. 2011 Jul 15; 286(28):24638–48. Epub 2011/05/18. eng. [PubMed: 21576245]
29. DiCamillo SJ, Carreras I, Panchenko MV, Stone PJ, Nugent MA, Foster JA, et al. Elastase-released epidermal growth factor recruits epidermal growth factor receptor and extracellular signal-regulated kinases to down-regulate tropoelastin mRNA in lung fibroblasts. J Biol Chem. 2002 May 24; 277(21):18938–46. Epub 2002/03/13. eng. [PubMed: 11889128]
30. Vandermeeren M, Daneels G, Bergers M, van Vlijmen-Willems I, Pol A, Geysen J, et al. Development and application of monoclonal antibodies against SKALP/elafin and other trappin family members. Arch Dermatol Res. 2001 Jul; 293(7):343–9. Epub 2001/09/12. eng. [PubMed: 11550807]
31. Foekens JA, Ries C, Look MP, Gippner-Steppert C, Klijn JG, Jochum M. The prognostic value of polymorphonuclear leukocyte elastase in patients with primary breast cancer. Cancer Res. 2003 Jan 15; 63(2):337–41. [PubMed: 12543785]
32. Maroulakou IG, Anver M, Garrett L, Green JE. Prostate and mammary adenocarcinoma in transgenic mice carrying a rat C3(1) simian virus 40 large tumor antigen fusion gene. Proc Natl Acad Sci U S A. 1994 Nov 8; 91(23):11236–40. Epub 1994/11/08. eng. [PubMed: 7972041]
33. Green JE, Shibata MA, Yoshidome K, Liu ML, Jorcyk C, Anver MR, et al. The C3(1)/SV40 T-antigen transgenic mouse model of mammary cancer: ductal epithelial cell targeting with multistage progression to carcinoma. Oncogene. 2000 Feb 21; 19(8):1020–7. Epub 2000/03/14. eng. [PubMed: 10713685]
34. Duncan JS, Whittle MC, Nakamura K, Abell AN, Midland AA, Zawistowski JS, et al. Dynamic reprogramming of the kinome in response to targeted MEK inhibition in triple-negative breast cancer. Cell. 2012 Apr 13; 149(2):307–21. Epub 2012/04/17. eng. [PubMed: 22500798]
35. Herschkowitz JI, Simin K, Weigman VJ, Mikaelian I, Usary J, Hu Z, et al. Identification of conserved gene expression features between murine mammary carcinoma models and human breast tumors. Genome biology. 2007; 8(5):R76. Epub 2007/05/12. eng. [PubMed: 17493263]
36. Robinson GW, Johnson PF, Hennighausen L, Sterneck E. The C/EBPbeta transcription factor regulates epithelial cell proliferation and differentiation in the mammary gland. Genes Dev. 1998 Jun 15; 12(12):1907–16. [PubMed: 9637691]
37. Jiang Z, Zacksenhaus E. Activation of retinoblastoma protein in mammary gland leads to ductal growth suppression, precocious differentiation, and adenocarcinoma. J Cell Biol. 2002 Jan 7; 156(1):185–98. [PubMed: 11777937]
38. Cole KA, Harmon AW, Harp JB, Patel YM. Rb regulates C/EBPbeta-DNA-binding activity during 3T3-L1 adipogenesis. American journal of physiology Cell physiology. 2004 Feb; 286(2):C349–54. Epub 2003/10/25. eng. [PubMed: 14576085]
39. Comprehensive molecular portraits of human breast tumours. Nature. 2012 Oct 4; 490(7418):61–70. Epub 2012/09/25. eng. [PubMed: 23000897]
40. Mainardi CL, Dixit SN, Kang AH. Degradation of type IV (basement membrane) collagen by a proteinase isolated from human polymorphonuclear leukocyte granules. J Biol Chem. 1980 Jun 10; 255(11):5435–41. Epub 1980/06/10. eng. [PubMed: 6989826]

41. Porter DC, Zhang N, Danes C, McGahren MJ, Harwell RM, Faruki S, et al. Tumor-specific proteolytic processing of cyclin E generates hyperactive lower-molecular-weight forms. Mol Cell Biol. 2001 Sep; 21(18):6254–69. [PubMed: 11509668]

42. Akli S, Van Pelt CS, Bui T, Meijer L, Keyomarsi K. Cdk2 is required for breast cancer mediated by the low-molecular-weight isoform of cyclin E. Cancer Res. 2011 May 1; 71(9):3377–86. Epub 2011/03/10. eng. [PubMed: 21385896]

43. Yang X, Yan H, Zhai Z, Hao F, Ye Q, Zhong B. Neutrophil elastase promotes proliferation of HaCaT cell line and transwell psoriasis organ culture model. International journal of dermatology. 2010 Sep; 49(9):1068–74. Epub 2010/10/05. eng. [PubMed: 20883273]

44. Huang CD, Chen HH, Wang CH, Chou CL, Lin SM, Lin HC, et al. Human neutrophil-derived elastase induces airway smooth muscle cell proliferation. Life sciences. 2004 Apr 2; 74(20):2479–92. Epub 2004/03/11. eng. [PubMed: 15010259]

45. Yang H, Zhou H, Feng P, Zhou X, Wen H, Xie X, et al. Reduced expression of Toll-like receptor 4 inhibits human breast cancer cells proliferation and inflammatory cytokines secretion. Journal of experimental & clinical cancer research: CR. 2010; 29:92. Epub 2010/07/14. eng. [PubMed: 20618976]

46. Shapiro SD, Goldstein NM, Houghton AM, Kobayashi DK, Kelley D, Belaaouaj A. Neutrophil elastase contributes to cigarette smoke-induced emphysema in mice. Am J Pathol. 2003 Dec; 163(6):2329–35. Epub 2003/11/25. eng. [PubMed: 14633606]

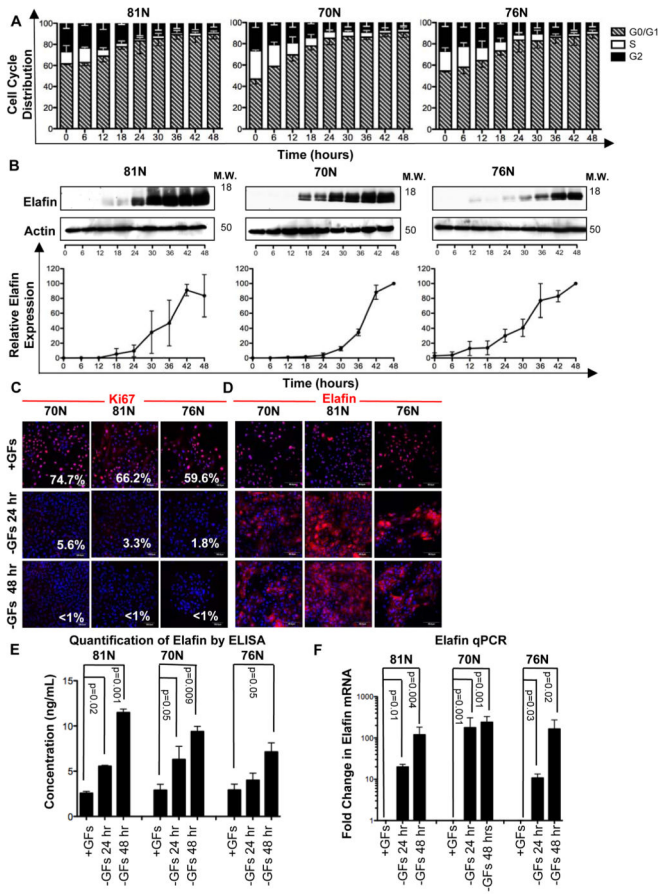

Figure 1. Elafin is Highly Expressed in Quiescent HMECs

(A, B) 81N, 70N, and 76N HMECs were cultured in growth factor (GF)-deficient medium and harvested every 6 hours for 48 hours (n=3 for each time point). (A) Cell cycle distribution determined by DNA content analysis. (B) Representative western blots of elafin expression. Actin, loading control. Elafin western blots were analyzed densitometrically; values were normalized and are displayed as a percentage of maximum expression. (C, D) 81N, 70N, and 76N HMECs were cultured with GFs (+GFs) for 24 hours or without GFs (−GFs) for 24 and 48 hours and examined by immunofluorescence staining for Ki67 (C) and elafin (D). Scale bars are 50 μm. (E) HMECs were cultured as described in C, conditioned media were collected and examined for elafin levels by ELISA. Concentrations are reported as ng of elafin per mL of medium. (F) HMECs were cultured as described in C and examined by qPCR for elafin expression; values were normalized to GAPDH and represented as a ratio to the control (+GFs condition).

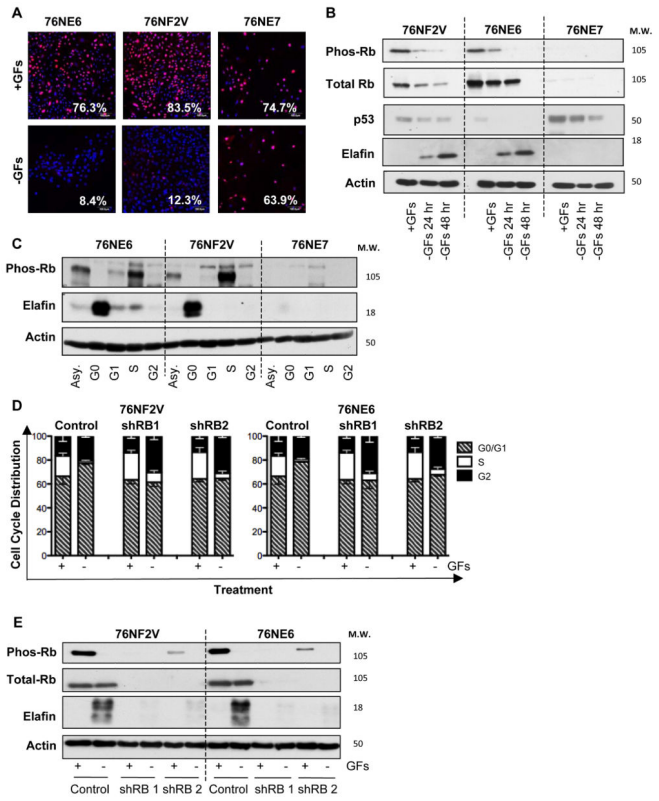

Figure 2. Rb-Deficient HMECs are Incapable of G0 Arrest and Fail to Upregulate Elafin

(A) 76NE6, 76NF2V, and 76NE7 immortalized HMECs were cultured with GFs (+GFs) or without GFs (−GFs) for 48 hours and examined by immunofluorescence staining for Ki67 expression. Scale bars are 50 μm. (B) Western blot of pRb S807/811, total Rb, p53, and elafin in HMECs cultured with GFs (+GFs) for 24 hours or without GFs (−GFs) for 24 and 48 hours. Actin, loading control. (C) HMECS were cultured in growth factor containing medium (asynchronous; Asy), in the absence of growth factors (arrested in G0), with 10 μM lovastatin (arrested in G1), with 10 μM aphidicolin (arrested in S phase), and with 5 μM nocodazole (arrested in M phase). Western blot of pRb S807/811, total Rb, and elafin expression. Actin, loading control. (D,E) 76NF2V and 76NE6 cells stably infected with pGIPZ lentiviral vectors containing control and two unique, RB-specific shRNAs were cultured with GFs (+GFs) or without GFs (−GFs) for 24 hours. (D) Cell cycle distribution was determined DNA content analysis. (C) Western blot of phosphorylated Rb (S807/811) and elafin in 76NE6, 76NF2V, AND 76NE7

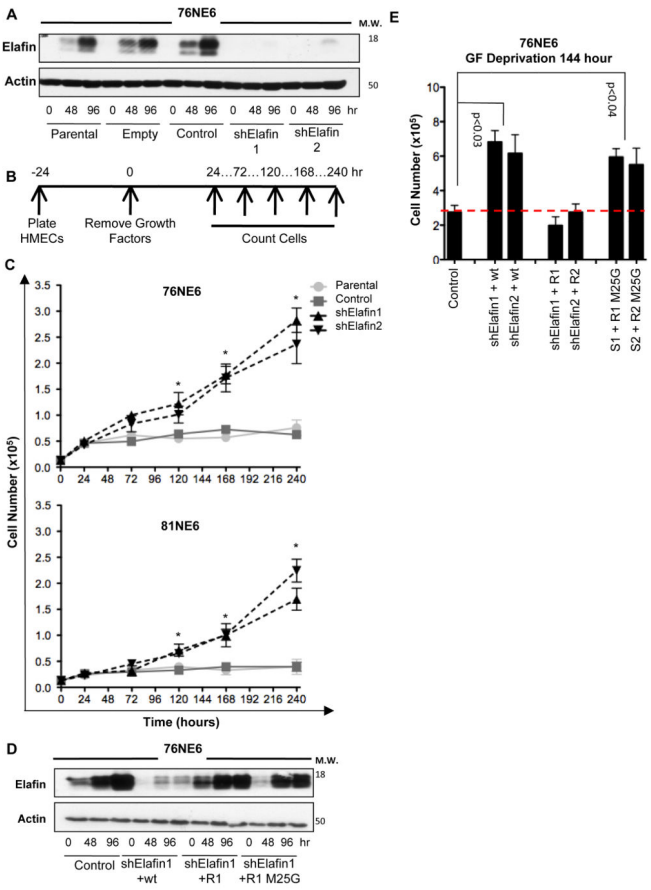

Figure 3. Elafin Knockdown HMECs Circumvent G0 Arrest and Proliferate in the Absence of Growth Factors (GFs)

(A) Western blot of elafin expression in parental, empty vector, non-targeting shRNA control, and elafin knockdown (shElafin 1 and shElafin 2) 76NE6 cells cultured with GF (0 hours) and without GFs for 48 and 96 hours. Actin, loading control. (B) Schematic of experimental design. 76NE6 cell lines from A were plated at an initial density of 2000 cells/well in 24-well plates and counted at the indicated times after growth factor removal. (C) Cell counts over time as described in B. Asterisks denote significant differences ($p<0.05$) between control and elafin-knockdown groups. (D) 76NE6 cells expressing elafin shRNA (shRNA1 [S1] and shRNA2 [S2]) were stably transduced with wild-type elafin (wt), shRNA-resistant elafin (R1, shRNA1-resistant elafin; R2, shRNA2-resistant elafin), or shRNA-resistant elafin with a M25G mutation (results for shRNA1 shown). Cell lysates were subjected to western blot analysis for elafin. Actin, loading control. (E) 76NE6 cells as described in D were cultured in the absence of GFs for 144 hours and counted.

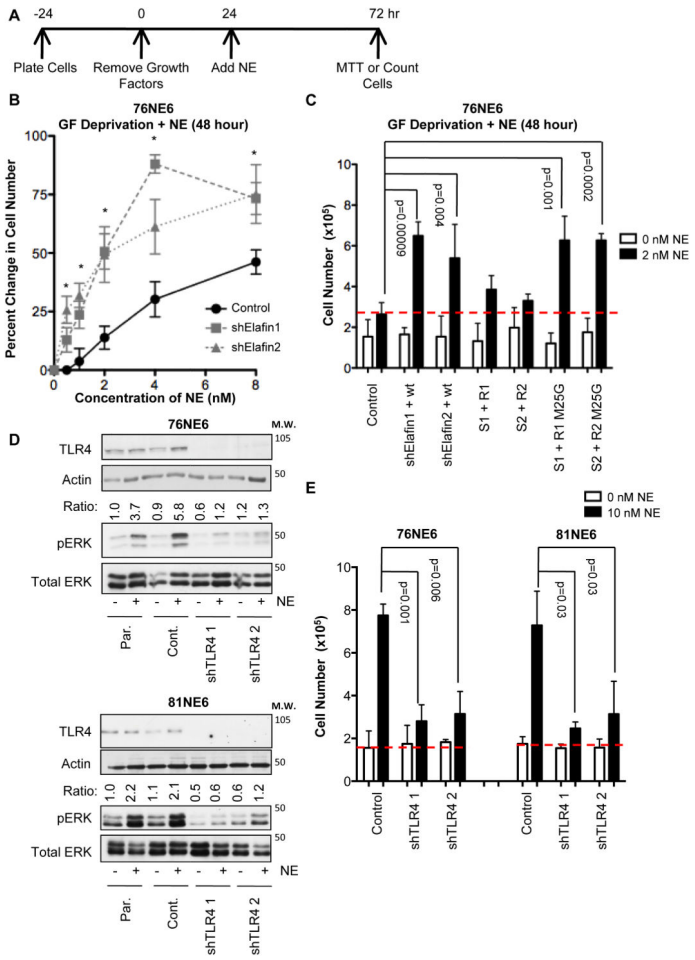

Figure 4. The Growth-Promoting Effect of Exogenous NE on G0 HMECs is Mediated by TLR4

(A) Schematic of experimental design. Cells were growth factor-deprived for 24 hours, and then exogenous NE (purified from human sputum) was added. Cell number was determined 48 hours after the addition of NE by either MTT assay or counting cells. (B) Elafin-knockdown and control 76NE6 cells were cultured in the presence of NE at the indicated concentrations, relative cell number was quantified by MTT assay 48 hours after the addition of NE. Asterisks denote significant differences ($p<0.05$) between control and elafin-knockdown cells. (C) 76NE6 cells described in Figure 3D were stimulated with 2 nM NE, and relative cell number was assessed 48 hours after the addition of NE. (D) Western blot analysis of TLR4 (actin as a loading control), pERK, and total ERK in 76NE6 and 81NE6 TLR4-knockdown cells GF deprived for 24 hours followed by stimulation with 10 nM NE. Par., parental. Cont, control. pERK/ERK ratio reported as in A. (E) 76NE6 and 81NE6 TLR4-knockdown cells were counted 48 hours after the addition of 10 nM NE as shown schematically in Figure 4A.

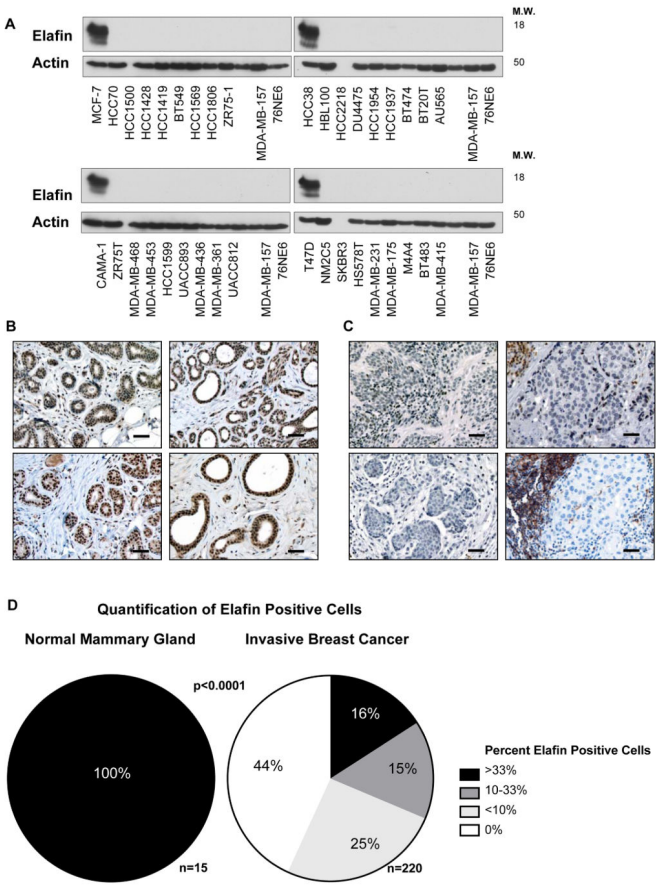

Figure 5. Elafin is Downregulated in the Majority of Breast Tumors

(A) Western blot analysis of elafin expression in 36 breast cancer cell lines compared to the immortalized HMECs, 76NE6. (B,C) Representative photomicrographs of elafin IHC staining in (B) normal breast tissue from reduction mammoplasty and (C) invasive breast carcinoma. Scale bar, 50μm. (D) Quantification of elafin expression in the normal mammary breast and invasive breast carcinoma tissue specimens. The frequency of elafin positive cells was estimated as a percentage of total cell number in representative tumor areas. These scores were categorized into four groups:0%, <10%, 10–33%, and >33%. Significance was determined by Fisher's Exact Test.

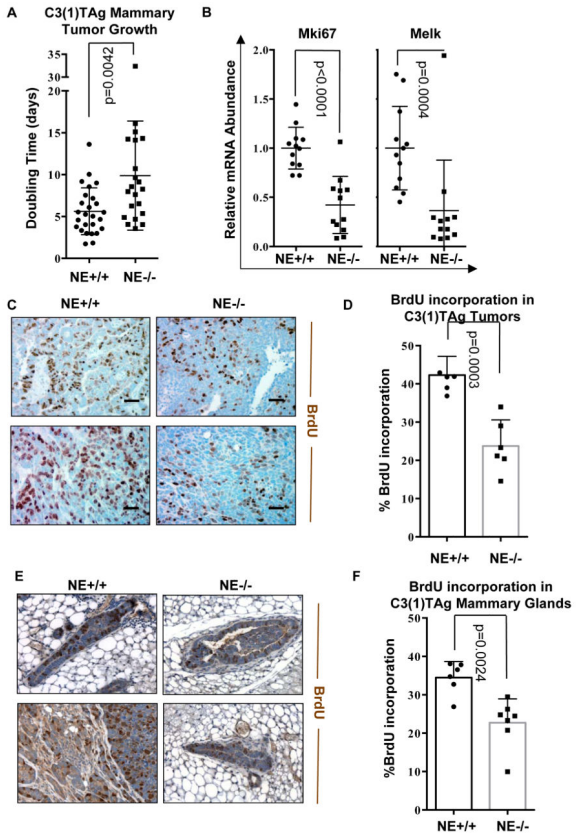

Figure 6. NE Knockout Reduces Tumor Growth and Proliferation in the C3(1)TAg Model of TNBC

(A) Doubling time was calculated for all C3(1)TAg NE+/+ and C3(1)TAg NE−/− tumors by fitting an exponential growth model. (B) qPCR was used to evaluated the levels of Melk and Mki67 in NE+/+ and NE−/− C3(1)TAg tumors. Twelve tumors were examined per group. (C) Tumors were subjected to IHC analysis of BrdU incorporation. Scale bar, 50μm. (D) BrdU positive cells were quantified as a percentage of total cells in three representative high magnification fields (40x) per tumor, a total of six tumors were examined per group. (E, F) NE knockout reduces proliferation in the contralateral mammary gland of C3(1)TAg tumor bearing mice. (E) Contralateral mammary glands of tumor bearing mice were subjected to IHC analysis of BrdU incorporation. Scale bar, 50μm. (F) BrdU positive cells were quantified as a percentage of total cells in three representative high magnification fields (40x) per tumor, a total of six mammary glands were examined per group.